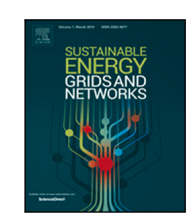
ELSEVIER

Contents lists available at ScienceDirect

## Sustainable Energy, Grids and Networks

journal homepage: www.elsevier.com/locate/segan





# A novel MILP formulation for optimal allocation and coordination of protective and switching devices in active distribution networks

Wandry Rodrigues Faria <sup>a</sup>, Gregorio Muñoz-Delgado <sup>b</sup>, Javier Contreras <sup>b,\*</sup>, Benvindo Rodrigues Pereira Jr. <sup>a</sup>

- <sup>a</sup> Department of Electrical and Computer Engineering, University of São Paulo, São Carlos SP, Brazil
- <sup>b</sup> Escuela Técnica Superior de Ingeniería Industrial, Universidad de Castilla-La Mancha, 13071 Ciudad Real, Spain

#### ARTICLE INFO

#### Keywords:

Control and protective device allocation Coordination and selectivity Distribution protection system planning MILP

#### ABSTRACT

In the last decade, the increasing penetration of distributed generation has prompted the proposal of new formulations for distribution protection system planning, as the typical indications of coordination may not be reliable for active networks. In this context, a few papers that explicitly enforce coordination constraints have been published. However, these papers are mostly based on heuristics and metaheuristics; therefore, although the solutions are feasible, there is no guarantee of optimality. This paper presents a mixed-integer linear formulation for the allocation and coordination of control and protective devices in distribution systems with distributed generators. Thus, the proposed approach guarantees both the optimal investment plan and feasibility of the protection system operation. The proposed formulation is tested for a 69-node system considering load restoration possibilities via island operation, using protective devices, and load transfer to neighboring feeders and fault permanent isolation, using switching devices. The results attest to the cost-effectiveness of the protection system and its operational feasibility, as well as the superiority of the proposed model over simpler existing ones.

#### 1. Introduction

The correct operation of the protection system is crucial to guarantee the safety of both people and equipment. Moreover, given that 80% of the entire power system's outage time is due to faults that occur in the primary feeders of distribution systems (DSs) [1], a selective protection system operation may significantly reduce outage time, leading to customer satisfaction maximization. In this sense, proposals addressing the optimization of the allocation and coordination of PDs, such as fuses, relays, and reclosers, and CDs, like manual and automatic switches, in DSs have been published for over 30 years [2]. Although some papers found in the literature focus solely on the allocation of either CDs or PDs, such as [3,4], the most common approach is to combine both into a single formulation.

In the context of radial DSs' protection systems, the allocation of PDs impacts the customers' satisfaction because the area affected by a fault can be contained by the closest upstream PD of the fault point. Nonetheless, this feature is subject to the protection system's coordination and selectivity, i.e., if the primary PD does not operate faster than its backup, the outage region will be larger than expected. Years of practice with traditional DSs (e.g., without reverse flow and

featuring ever-decreasing currents the further a branch is from the substation) have allowed engineers and distribution companies (DIS-COs) to create empirical rules that usually ensure coordination and selectivity between PDs. Such rules were integrated into more complex models for protection system planning [5-8]. The authors of [5,6] have proposed mixed-integer nonlinear programming (MINLP) approaches for the allocation of fuses and automatic switches (ASs). The allocation of these devices was optimized to maximize the protection system cost-effectiveness, i.e., minimization of expected cost of energy not supplied (ECENS) plus investment costs. These models were expanded in [7-9] to account for the allocation of reclosers. The authors of [7] developed a MINLP formulation of the optimization problem, while the authors of [8,9] elaborated a mixed-integer linear programming (MILP) model, for which finite convergence to the optimal solution is guaranteed. Approaches [5-9] also consider maneuvering ASs to permanently isolate a faulty section followed by a reclosing maneuver as a means to restore load after an outage event, which we will refer to as fault isolation maneuver (IM) hereinafter. Moreover, the authors of [5,6], and [8] account for load transferring between neighboring

E-mail addresses: wandry@usp.br (W.R. Faria), gregorio.munoz@uclm.es (G. Muñoz-Delgado), javier.contreras@uclm.es (J. Contreras), brpjunior@usp.br (B.R. Pereira Jr.).

<sup>\*</sup> Corresponding author.

### Nomenclature

The number of branches in a radial network is equal to the number of nodes plus one; thus, it is possible to enumerate the branches with the same number as the bus connected to the branch's end terminal. Adopting this enumeration pattern, we use the same indexes for lines and branches. Furthermore, we use the term "branch i" to refer to the branch whose end terminal is node i.

#### Sets

Set of fault types such that $\Delta = \{P, T\}$
(namely, permanent and temporary faults).
Set of years in the planning horizon.
Sets of fuse capacity and recloser time-
inverse curves (namely, inverse, very in-
verse, and extremely inverse).
Set of types of customers.
Set of distribution nodes.
Sets of distribution nodes downstream of
node $i$ including and disregarding node $i$ .
Sets of distribution nodes upstream of node
i including and disregarding node i.

; ,;	node $i$ including and disregarding node $i$ .
$\varOmega^u_i, \varOmega^{u*}_i$	Sets of distribution nodes upstream of node <i>i</i> including and disregarding node <i>i</i> .
Indices	
a, b	Indices for fuse capacity.
c,d	Indices for recloser time-inverse curves.
i, j, k, f	Indices for nodes/branches.
t	Index for the type of customer (residential, commercial, and industrial).
w	Index for the fault type.
y	Index for years.
Parameters	

Parameters used to calculate the recloser's

# Parameters $A_c, B_c, \mathcal{R}_c$

C. C. C	acting time under inverse curve $c$ .
$A_{ij},  ilde{A}_{ij}$	Incidence matrix and negative-
.,· .,	inverse-transposed incidence
	matrix.
$C^{AA}, C^{AI}$	Costs for the acquisition of switches and
	islanding devices.
$C^{AF}, C^{AR}$	Costs for the acquisition of fuses and
	reclosers.
$C^{MA}, C^{MI}$	Costs for the maintenance of switches and
	islanding devices.
$C^{MF}, C^{MR}$	Costs for the maintenance of fuses and
	reclosers.
$\underline{I}_{ii}^{scc}, \overline{I}_{ii}^{scc}, I_i^{pu}$	Minimum and maximum short-circuit cur-
_,, ., .	rent measured at branch i for a fault at
	branch $j$ and pick-up current of the recloser
	located at branch i.
IRR	Internal rate of return.
M	Sufficiently large positive value used for
	linearization purposes.
$P_{iy}$	Total demand downstream of node i (in-
	cluding node i) at year y.
$P_{tiy}$	Total demand of type t customers down-
	stream of node $i$ (including node $i$ ) at year
	у.

$P_{iy}^{DG},P_{iy}^{NF}$	Capacity of the generator and neighboring feeder connected to node $i$ at year $y$ .
$\underline{R}^t$	Minimum tripping time for reclosers.
$T_i$	Type of branch: 0 for the main feeder and paths connecting the substation and generators and 1 otherwise.
$T_{ija}^{f-min}, T_{ija}^{f-max}$	Minimum and maximum acting time of a fuse with capacity $a$ installed at branch $i$ for a fault at branch $j$ .
$\kappa^{(*)}$	Coordination factors for protective devices.
$\lambda_{iw}$	Expected number of type $w$ faults occurring at the branch upstream of node $i$ per year.
$Y_w$	Expected outage duration (repair time) for a fault of type $\it w$ .
$\phi_t$	Interruption costs of a type t customer.
τ	Maximum acting time for a protective device to clear a fault within its primary protection zone.

#### **Binary Variables**

$x_i^{AS}, x_i^{LT}$	Variables that indicate the allocation of an automatic switch at branch <i>i</i> and whether or not such device is able to perform load-transferring maneuvers, respectively.
$x_{ia}^{FS}, x_{ia}^{FB}$	Variables that indicates the allocation of a type <i>a</i> fuse employing fuse-save and fuse-blow schemes at branch <i>i</i> .
$x_i^{ID}$	Variable that indicates the allocation of an islanding device at branch <i>i</i> .
$x_{ic}^{RD}$	Variable that indicates the allocation of a recloser with time-inverse curve $c$ at branch $i$ .
$z_{ij}$	Variable that indicates that the only protective device between branches $i$ and $j$ is located at branch $i$ .
$z_{ij}^0$	Variable that indicates that there is no protective device between branches $i$ and $j$ , nor at branches $i$ and $j$ .
$z_{ijf}^{AS}$	Variable that indicates that the automatic switch located at branch $j$ must operate to isolate a fault at branch $f$ after it has been cleared by the protective device installed on branch $i$ .
$z_{ij}^{FB}$	Variable that indicates that the only protective device between branches $i$ and $j$ is a fuse-blow device located at branch $i$ .
$z^R_{ij}$	Variable that indicates that the only recloser between branches $i$ and $j$ is located at branch $i$ .

#### **Continuous Variables**

$C^A, C^M$	Total acquisition and maintenance costs.
$C^T$	Total cost.
CENS	Total expected cost of energy not supplied.
$e_{iwy}^{ENS}$	Energy not supplied due to the operation of a protective device located at branch $i$ to eliminate a fault of type $w$ at year $y$ .
$e_{iy}^{IO}, e_{iy}^{LT}, e_{iy}^{IM}$	Energy restored via island operation, load transfer, and fault isolation maneuver at year $y$ due to the operation of a device located at branch $i$ .

$p_{iy}^{IO}, p_{iy}^{LT}, p_{iy}^{IM}$	Power restored via island operation, load transfer, and fault isolation maneuver at year $y$ due to the operation of a device located at branch $i$ .
$t_{ic}^{dial}$	Time-dial setting of the recloser located at branch $i$ under inverse-time curve $c$ .
t <sup>rd-min</sup> , t <sup>rd-max</sup> ijc tijc	Action time of the recloser located at branch $i$ operating under inverse-time curve $c$ for the maximum and minimum short-circuit current measured for a fault at branch $j$ , respectively.
$t_i^{RF}$	Time-defined action of recloser at branch $i$ .
$ ho_{ijfy}, \epsilon_{jf}$	Auxiliary variables employed to calculate the total power and energy restoration due to fault isolation maneuvers, respectively.
$\chi_i, z_i$	Binary-valued continuous variables that indicate, respectively, the presence and absence of any protective device at branch <i>i</i> .
$\chi_i^F$	Binary-valued continuous variable that indicates the presence of a fuse at branch <i>i</i> .
$\chi_i^{FS}, \chi_i^{FB}$	Binary-valued continuous variables that indicate the allocation of fuses adopting fuse-save and fuse-blow schemes, respectively, at
$\chi_i^R$	branch <i>i</i> .  Binary-valued continuous variable that indicates the presence of a recloser at branch <i>i</i> .

feeders, which we will refer to simply as load transferring maneuver (LT) in this paper. Unfortunately,[6–9] fail to account for the mere presence of distributed generators (DGs), which is part of the reality of most DSs nowadays. Furthermore, the authors of [5–9] disregard coordination constraints. It is important to highlight that coordination between PDs is the fundamental assumption upon which the ECENS is calculated.

The authors of [10-13] have addressed the allocation of CDs and PDs in DSs with DGs. In all of these approaches, the island operation (IO) and IM are considered as possibilities to restore load after an outage event. The formulations shown in [12,13] also allow LT. Except for the approach presented in [13], all of these optimization problems were solved using heuristic and metaheuristic algorithms that cannot attest to the optimality of the solution. Furthermore, as a general rule, the installation of DGs in a DS leads to coordination failure between PDs [14]. Thus, formulations that account for the presence of DGs usually feature additional coordination constraints, as attaining it becomes more challenging. Unfortunately, approaches [10-13] lack coordination constraints other than imposing a limit for the number of reclosers in the DS or the number of series fuses, i.e., the actual operating time of each PD for each fault event is not calculated. It should be stressed that the kind of constraints employed in [10-13] may not be enough to ensure the coordination of PDs in DSs with DGs, especially when there are fuses operating under the fuse-save scheme, as shown in [15]. In this sense, none of the approaches mentioned thus far can attest to their operational feasibility, given that coordination is not actively verified. Therefore, the expected costs and reliability indexes obtained by such methods may not be observed in real-world applications.

This brief review of the recent literature allows one to notice that, although the allocation and coordination of PDs are intertwined problems, it is not unusual to find (1) proposals for the optimized allocation of PDs that do not directly verify the coordination constraints [5–8,

Table 1
Comparison of contributions.

Paper	Consideration						
	FBA	CSA	IO	LT	IM	OAC	
[5,6]	Х	Х	Х	/	/	Х	
[7]	/	X	Х	X	✓	Х	
[8]	/	Х	Х	1	1	Х	
[9]	/	X	Х	X	✓	Х	
[10,11]	/	X	✓	X	✓	Х	
[12]	X	Х	1	1	1	Х	
[13]	/	X	✓	✓	✓	Х	
[21,22]	X	✓	✓	✓	Х	Х	
[23,24]	/	✓	✓	✓	Х	Х	
This paper	/	✓	✓	✓	✓	✓	

Note: FBA — fuse-blow allocation; CSA — coordination and selectivity assessment; IO — load restoration via island operation; LT — load restoration via load transfer; IM — load restoration via faulty section isolation using ASs; OAC — optimal allocation and coordination of CDs and PDs.

10–13], and (2) complementary methods addressing exclusively the coordination of existing PDs in a DS [16–20].

Few approaches, such as [21-24], have considered the allocation of PDs in DSs with DGs while regarding coordination between the PDs as constraints. The combination of these problems (i.e., allocation and coordination) leads to a non-convex MINLP formulation, which, due to its complexity, is solved by multi-objective genetic algorithms (MOGAs) in [21-23] and by a matheuristic approach (composed by a MILP model nested within a MOGA) in [24]. It should be pointed out that approaches [21-24], despite regarding both problems, solve them in two phases rather than simultaneously, e.g., first, candidate solutions (i.e., protection topologies) are created via genetic operators, and, then, a coordination problem is solved for each protection system topology using heuristics, metaheuristics or MILP. Thus, despite being able to attest to the feasibility of the protection system topology, proposals [21-24] depend on heuristic and metaheuristic tools to explore the optimization problem's search space. Therefore, there is no optimality guarantee nor estimation of how far a solution is from the optimal value for none of these approaches, given that the allocation and, in Refs. [21-23], also the coordination, may not be optimal.

In this context, we propose a novel formulation to bridge the above-described gaps found in the relevant literature regarding the allocation of control and protective devices in DSs with DGs, which cannot be found in [5–13,16–24]. The proposed model integrates the allocation and coordination of reclosers, fuses (operating under both fuse-save and fuse-blow schemes), islanding devices (IDs), and ASs in a single problem. Moreover, the proposed model is formulated as a MILP for which finite convergence to optimality is guaranteed, thus avoiding all of the optimality-related shortcomings observed in [21–24] while maintaining the contributions provided by these papers. We also consider the possibility of using IDs to enable IO, as well as the use of ASs to perform LT and IM as means to restore healthy out-of-service areas and minimize the impacts of outage events. A comparison between this proposal and relevant approaches found in the literature is provided in Table 1, which highlights the following main contributions of this article:

- Optimizing allocation of PDs considering coordination constraints to guarantee operational feasibility, which is not available in [5–13,16–20];
- 2. Allocation of protective and controlling devices taking into account their impact on multiple possibilities of load restoration after fault events (namely IO, LT, and IM) as a means to minimize the ECENS. Only approaches [12,13] account for all of these load restoration methods; however, the two fail to verify coordination between PDs, which may render such maneuvers infeasible or ineffective;

3. Development of a MILP formulation to ensure finite convergence to optimality for the allocation problem while considering coordination between PDs as a constraint, which is not available in [5–13,16–24].

The remainder of this paper is divided into four sections; in Section 2, we provide the assumptions and protection philosophies adopted to develop the optimization model presented in this paper; Section 3 provides the optimization problem for the minimization of investment costs plus ECENS (i.e., cost-effectiveness maximization) taking into account the allocation of CDs and PDs and the coordination between the allocated PDs; numerical results obtained using the proposed formulation are provided in Section 4; finally, the conclusions are drawn in Section 5.

# 2. Considerations regarding protection system design for active distribution networks

In this paper, we consider the allocation of reclosers and IDs (digital PDs), fuses (analog PDs), and ASs (CDs). It should be highlighted that, although overcurrent relays are not explicitly considered in this formulation, the constraints used to describe the operation and coordination of reclosers could be applied to represent relays. From a formulation standpoint, the consideration of reclosers and relays are equivalent as the constraints would not change, albeit the costs associated with purchasing and maintaining reclosers and relays could vary. In this section, we present the assumptions adopted in this paper. For the sake of compactness, only a brief explanation regarding the coordination philosophy is presented; nonetheless, more detailed descriptions of how a PD coordinates with other PDs can be found in [21].

#### 2.1. Adopted protection philosophies and restoration possibilities

As a general rule, the coordination between two PDs is selective, i.e., the one closest to the fault must operate, limiting the outage area to a minimum. However, we consider two schemes for the coordination of a fuse and a recloser, namely fuse-save and fuse-blow. In the first one, the recloser (further from the fault location) must operate faster than the fuse in their fast action, which is not selective as the affected area is greater; nonetheless, the recloser automatically restores the power supply after a few seconds, and, if the fault has naturally been cleared, there is no permanent outage. If the fault persists, the recloser's delayed action must take longer to operate than the fuse, thus guaranteeing selectivity in case of a permanent fault. As for the fuse-blow scheme, the operation is always selective, i.e., the recloser never operates before the fuse. As a result, the area downstream of the fuse will suffer permanent outage even if the fault event is temporary.

Once the outage area, which depends on the location of both the fault and the PD that clears the fault, is determined, it is possible to formulate and execute service restoration plans. In this approach, and in consonance with previous research as shown in Table 1, we consider IO, LT, and IM as means for load restoration. The IDs are used solely to enable IO while ASs can be used only to perform LT and IM.

As considered in [21–23], we regard the IDs as an overcurrent relay with a directional unit that allows the PD to operate only for upstream faults. In this sense, the islanding region is defined as the area downstream of the ID that operates disconnected from the main grid whenever there is a fault out of the islanding region. Thus, the ID does not coordinate with any other PD since it must operate as fast as possible whenever the fault is out of the islanding region, regardless of the actions of other PDs. Alternatively, if the fault is inside the islanding region, the ID does not operate, regardless of the actions of other PDs. It is important to stress that DGs typically possess local protection systems that monitors voltage and frequency variations. Hence, changing the operation mode from grid connected to island cannot cause abrupt oscillations otherwise the DG's local protection may trip. Previous

works have shown that careful setting the DG power dispatch and the load switching in and out of the island can ensure the maintenance of the island mode [25].

The ASs cannot be used to clear faults; however, once the fault has been cleared, the areas affected by the outage can be restored by maneuvering ASs. One way to do so is via LT, which is possible if the fault is upstream of the AS and there is a neighboring feeder downstream of this AS with enough capacity to supply the load downstream of the AS. The second possibility considered in this paper is IM, which is possible whenever the fault is downstream of the AS and a recloser (located upstream of the AS) is responsible for clearing a permanent fault, i.e., the recloser is the first PD upstream of the fault location. In this case, the AS can be opened to permanently isolate the fault. Then, the recloser is maneuvered to resupply the downstream loads. Observe that, in the first restoration possibility using ASs, the load downstream of the AS is restored, and, in the second, the load downstream of the recloser and not downstream of the AS is restored.

Finally, it is important to highlight some limitations of the proposed approach. Firstly, the consideration that the IDs must trip for every upstream fault as soon as possible may lead to unnecessary islanding maneuvers as some faults could be cleared without such action. Nonetheless, by doing so we avoid the possibility of disconnecting the DG due to the operation of its local protection system [26]. Secondly, the maintenance of the island operation depends on the instantaneous power balance between the local generation and demand at the moment of the island formation [25]. We assume that the balance will always be met (or present a close enough mismatch) and, as a result, the island operation will always be successful.

#### 2.2. Summary of assumptions and definitions regarding PDs and CDs

The definitions and operational possibilities of the protective and controlling devices addressed in this paper are as follows. Fuses and reclosers are PDs responsible solely for clearing faults downstream of their location; IDs are PDs responsible solely for clearing faults upstream of their location and thus putting the downstream DGs under island operation (IO); ASs are CDs (that can be operated only after an upstream PD has cleared the fault) responsible for allowing load transfer between neighboring feeders (LT) and permanently isolating downstream faults (IM).

The assumptions considered in [21,22] regarding the characteristics and abilities of each device (listed below) are granted in this approach.

- reclosers and IDs possess directional units and operate for faults in a single direction, i.e., reclosers operate for downstream faults and IDs act for upstream faults;
- 2. the allocation of a recloser implies setting the device's fast and delayed operations. We consider a time-defined action (ANSI 50) for the fast action. As for the delayed action (ANSI 51), we consider three inverse-time curve (ITC) options, namely, inverse, very inverse, and extremely inverse;
- 3. setting a recloser's delayed action implies determining not only the ITC but also the pick-up current and time dial [27].
- since IDs must operate for every fault out of the island region regardless of the existence of other PDs, coordination with upstream PDs is not necessary;
- 5. DGs possess local protective devices responsible for clearing faults inside the islanding region. It is important to mention that modeling and setting such PDs is not within the scope of this paper but can be found in [23];

<sup>&</sup>lt;sup>1</sup> It should be stressed that the term "not downstream" cannot be replaced by "upstream" as not every node downstream of the recloser is necessarily upstream of the AS. Moreover, it is not accurate to employ the expression "between" the recloser and the AS to describe the region restored by IM, as lateral feeders downstream of the recloser are not physically between the recloser and the AS but are indeed restored by this maneuver.

6. IO can be performed only by IDs (and restores downstream loads) while LT and IM can only be performed by ASs (and restores, respectively, loads downstream of the AS and loads comprised downstream of the recloser responsible for clearing the fault and not downstream of the AS that performs the maneuver).

#### 3. Proposed mathematical model

The assessment of distribution networks' protection systems is typically conducted taking into account investment costs and reliabilityrelated indices. Usually, such analysis takes into account system average interruption duration index (SAIDI) and ECENS indices since the operation of PDs to eliminate fault currents usually provokes energy outage areas that affect these values. In this paper, we consider ECENS and investment costs as parameters to evaluate the protection system, as the two share the same unit (\$) and can be added into a single objective function without any weighting factor. This section is divided into six parts. The first addresses investment cost formulation as a function of allocation and coordination constraints; the second presents the constraints adopted in this paper regarding the allocation and coordination of PDs and CDs; next we develop a mathematical formulation for expressing ECENS as a function of the allocation and coordination constraints; in the fourth part, we present the formulation used to account for restoration possibilities (i.e., IO, LT, and IM); the complete MILP formulation is shown in the fifth part; finally, the last subsection shows an illustrative example of how the proposed constraints work considering a small DS.

#### 3.1. Investment cost calculation

The investment cost is associated with the acquisition and maintenance costs of CDs and PDs. The existing literature has vastly explored its formulation as a function of the allocation problem's decision variables [21]. In line with existing formulations, the total investment cost is calculated as shown in (1). Two components for the total investment cost, namely the acquisition and maintenance costs (calculated in (2) and (3)), are considered.

$$C^T = C^A + C^M \tag{1}$$

$$C^{A} = \sum_{i \in O} C^{AF} \chi_{i}^{F} + C^{AR} \chi_{i}^{R} + C^{AI} \chi_{i}^{ID} + C^{AA} \chi_{i}^{AS}$$
 (2)

$$C^{M} = \sum_{y \in \mathcal{H}} \sum_{i \in O} \frac{C^{MF} \chi_{i}^{F} + C^{MR} \chi_{i}^{R} + C^{MI} \chi_{i}^{ID} + C^{MA} \chi_{i}^{AS}}{(1 + IRR)^{y}}$$
(3)

#### 3.2. Allocation and Coordination of PDs and CDs

As a general rule, PDs are coordinated by pairs in the sense that, by the end of the coordination process, every PD operates faster than any other upstream PD for a given downstream fault, thus guaranteeing that the primary PD acts before the backup device. It is possible to mathematically model this constraint by ensuring that every PD operates slower than any downstream PD instead of determining pairs of devices. Ruling whether or not a PD located at branch *j* is downstream of another PD situated at branch i can be easily done for a radial network using the reduced branch-node incidence matrix (A)2 and its negative transposed inverse (A) [28,29]. The number of branches

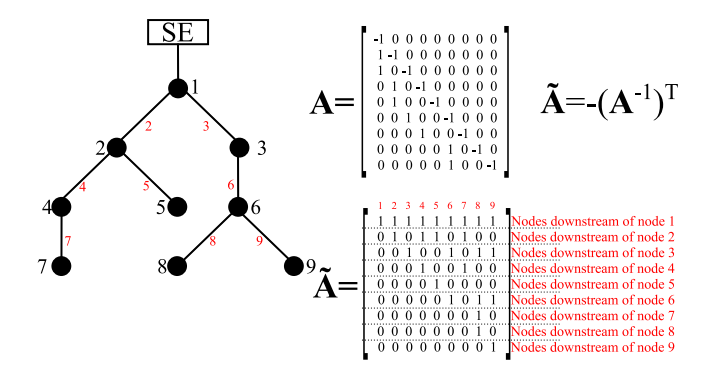


Fig. 1. Incidence matrix of a 9-node radial system.

and nodes in a radial network is the same; thus, it is possible to enumerate the branches with the same number as the bus connected to the branch's end terminal. Adopting this enumeration pattern,  $\tilde{\mathbf{A}}_{ij}=\mathbf{1}$ indicates that node j is downstream of node i. An illustrative example of this feature is shown in Fig. 1.

Hence, it is possible to use A to determine whether or not two devices must operate coordinately, i.e., if  $\tilde{A}_{ij} = 1$  the path that connects the substation and branch j passes through branch i and, therefore, the PDs located at these branches need to coordinate. Observe that the application of such method is not limited to pairs of PDs. In fact, every PD must coordinate with every other PD located in the path that connects to the substation. However, if  $\tilde{A}_{ij} = 0$ , then the operation of one of the PDs does not affect the other since the path that connects branch j to the substation does not include branch i. Thus, coordination between these PDs is unnecessary. Henceforth, we will refer to the set of branches downstream of branch i, i.e.,  $j \in \{N | \tilde{A}_{ij} = 1\}$ , as  $\Omega_i^d$  and to the set of nodes upstream of branch i, i.e.,  $j \in \{N | \tilde{A}_{ii} = 1\}$ , as  $\Omega_i^u$ . Whenever branch *i* is not to be included in the set, we will use  $\Omega_i^{d*}$  and  $\Omega_i^{u*}$ . Thus, the coordination problem can be written as a function of the allocation problem as follows.

$$\chi_i^{FB} = \sum_{a \in \mu^a} x_{ia}^{FB} \quad \forall i \in \Omega$$
 (4)

$$\chi_i^{FS} = \sum_{a \in u^a} \chi_{ia}^{FS} \quad \forall i \in \Omega$$
 (5)

$$\chi_{i}^{F} = \chi_{i}^{FB} + \chi_{i}^{FS} \quad \forall i \in \Omega$$
 (6)

$$\chi_i^F = \chi_i^{FB} + \chi_i^{FS} \quad \forall i \in \Omega$$

$$\chi_i^R = \sum_{c \in \mathcal{U}^d} \chi_{ic}^{RD} \quad \forall i \in \Omega$$
(6)

$$\chi_i = \chi_i^F + \chi_i^R \quad \forall i \in \Omega$$
 (8)

$$\chi_i + \chi_i^{AS} + \chi_i^{ID} \le 1 \quad \forall i \in \Omega$$
 (9)

$$x_i^{LT} \le x_i^{AS} \quad \forall i \in \Omega \tag{10}$$

$$0.05\chi_i^R \le t_i^{RF} \le \chi_i^R \quad \forall i \in \Omega$$
 (11)

$$\sum_{c \in \mu^d} t_{ijc}^{rd-min} \ge \kappa^{51-51} + \sum_{d \in \mu^d} t_{jjd}^{rd-max} \quad \forall i \in \Omega, j \in \Omega_i^{d*}$$
 (12)

$$\sum_{c \in \mu^d} t^{rd-min}_{ijc} \geq \kappa^{51-F} + \sum_{a \in \mu^a} (x^{FB}_{ja} + x^{FS}_{ja}) T^{f-max}_{jja}$$

$$\forall i \in \Omega, j \in \Omega_{i}^{d*}$$

$$(x_{ia}^{FB} + x_{ia}^{FS}) T_{ija}^{f-min} \ge \sum_{b \in \mu^{a}} \kappa^{F-F} (x_{jb}^{FB} + x_{jb}^{FS}) T_{jjb}^{f-max}$$
(13)

$$\forall i \in \Omega, j \in \Omega_i^{d*}, a \in \mu^a \tag{14}$$

$$t_i^{RF} \ge \kappa^{50-50} + t_j^{RF} \quad \forall i \in \Omega, j \in \Omega_i^{d*}$$
 (15)

$$t_{i}^{RF} \geq \sum_{a \in \mu^{a}} \kappa^{50-F} x_{ja}^{FB} T_{jja}^{f-min} \quad \forall i \in \Omega, j \in \Omega_{i}^{d*}$$

$$t_{i}^{RF} \leq \sum_{a \in \mu^{a}} \kappa^{50-F} x_{ja}^{FS} T_{jja}^{f-min} \quad \forall i \in \Omega, j \in \Omega_{i}^{d*}$$

$$(16)$$

$$t_i^{RF} \le \sum_{a \in u^a} \kappa^{50-F} x_{ja}^{FS} T_{jja}^{f-min} \quad \forall i \in \Omega, j \in \Omega_i^{d*}$$

$$\tag{17}$$

<sup>&</sup>lt;sup>2</sup> The branch-node matrix is composed of 0, 1 and -1.  $A_{ij} = 1$  indicates that j is the sending end of line i,  $A_{ij} = -1$  indicates that j is the receiving end of line i and  $A_{ij} = 0$  indicates that j is neither the sending nor the receiving end of line i. Considering a radial topology, the original branch-bus matrix is an N-1xN matrix, being N the number of nodes. Therefore, the matrix is not invertible. The reduced matrix does not consider the sending node of the first line, i.e., the substation node. Thus, A becomes an NxN invertible matrix.

$$t_{ijc}^{rd-min} = \left(\frac{A_c}{\left(\frac{\overline{I}_{ijc}^{scc}}{I_i^{pu}}\right)^{R_c} - 1} + B_c\right) t_{ic}^{dial}$$

$$\forall i \in \Omega, j \in \Omega_i^{d*}, c \in \mu^d$$

$$(18)$$

$$t_{ijc}^{rd-max} = \left(\frac{A_c}{\left(\frac{I_{ijc}^{sec}}{I_{ip}^{pu}}\right)^{R_c} - 1} + B_c\right) t_{ic}^{dial}$$

$$\forall i \in \Omega, j \in \Omega_i^{d*}, c \in \mu^d \tag{19}$$

$$0.01x_{ic}^{RD} \le t_{ic}^{dial} \le 100x_{ic}^{RD} \quad \forall i \in \Omega, c \in \mu^d$$
 (20)

$$t_{iic}^{rd-min} \ge \underline{R}^t \quad \forall i \in \Omega, c \in \mu^d$$
 (21)

The combination of (4)–(9) ensures that no more than one device, either protective or controlling, can be installed in a branch. Constraint (10) enforces that an AS must be allocated in branch i in order to allow the existence of a device able to perform LT, i.e.  $x_i^{LT}$ . The existence of a fast-acting protection function in a recloser installed at branch i is conditioned to the existence of an ITC at the same branch (assumption (3) as expressed in (11) combined with (7). Finally, the coordination constraints that ensure that the backup PDs' response takes longer than the primary device's considering the delayed operation of two reclosers, a recloser and a fuse, or two fuses are shown in (12)–(14), respectively. Notably, the acting time of the PDs whose primary protection zone include branch j are represented on the right-hand side of constraints (12)–(14). Thus, their action time must be lower than the backup PD, whose acting time is represented on the left-hand side of constraints (12)–(14).

The coordinated operation of two digital PDs' (i.e., reclosers) fast operation, as well as the consideration of fuse-blow and fuse-save schemes, are regarded in (15)–(17), respectively. Observe that, for the fuse-save scheme, i.e., (17), the backup PD's (recloser's) acting time (represented in the left-hand side of (17)) is lower than the primary device's (i.e., the fuse) as opposed to the formulations shown in (15)–(16). Thus, whenever there is a temporary fault, a fuse operating under the fuse-save scheme will not melt since the backup recloser will operate first, and the automatic reclosing maneuver will restore every consumer. Such scenario does not happen if the fuse-blow scheme, represented in (16), is adopted. In this case, the fuse's acting time is lower than the recloser's, thus the fuse will melt to clear a temporary fault, and the only way to restore the outage region is to replace the fuse. Finally, the delayed acting time of the reclosers is defined in (18)–(21).

Observe that constraints (12)–(17) could be considered for every set of two branches if not by the use of matrix **A** and the consequential determination of  $\Omega_i^d$  and  $\Omega_i^u$ . Thus, this formulation could also be applied to meshed distribution systems if a different type of incidence matrix were considered. As long as the operational topology (or multiple topologies) is known, the set of branches that at which coordination relationship should be observed can be determined; hence, the set of constraints can be correctly written.

It should be mentioned that in real-world applications, other allocation constraints are considered, such as (1) fuses cannot be allocated in the path connecting a DG and the substation to avoid bidirectional current flow in these PDs; (2) reclosers cannot be allocated downstream of fuses as a means to improve the network's reliability; and (3) IDs cannot be connected in series. Finally, from a safety perspective, setting an upper limit for the acting time of every PD considering a fault within its protection zone may be desirable[21,24]. All of the constraints mentioned in this paragraph are also taken into account in the proposed model as shown, in this order, in (22)–(25).

$$\chi_i^F \le T_i \quad \forall i \in \Omega \tag{22}$$

$$\chi_i^F \le 1 - \chi_j^R \quad \forall i \in \Omega, j \in \Omega_i^{d*}$$
 (23)

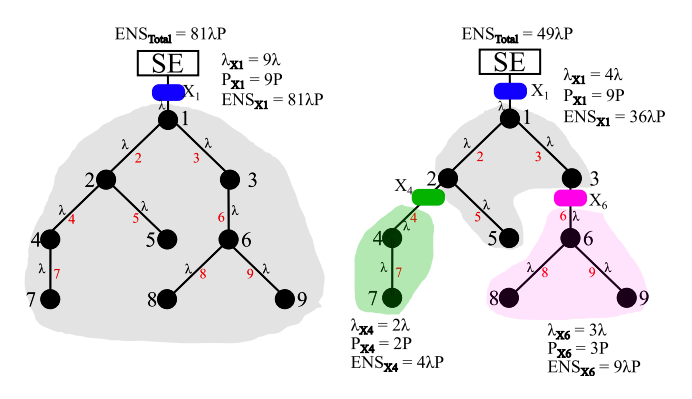


Fig. 2. Illustrative example of the effects of PD allocation in ENS calculation.

$$x_{i}^{ID} \leq 1 - x_{j}^{ID} \quad \forall i \in \Omega, j \in \Omega_{i}^{d*}$$

$$\sum_{a \in \mu^{d}} \left( x_{ia}^{FS} + x_{ia}^{FB} \right) T_{ija}^{f-max} + \sum_{c \in \mu^{d}} x_{ic}^{RD} t_{ijc}^{rd-max} \leq \tau$$
(24)

$$\forall i \in \Omega, j \in \Omega_i^{d*} \tag{25}$$

#### 3.3. Energy not supplied expected cost calculation

Considering that the protection system operates coordinately, which is assured by (12)–(17), and disregarding the possibility of load restoration, the area affected by a PD's operation is determined as the set of nodes downstream of the PD's location. However, the reliability indices are affected not only by an event's magnitude (i.e. size and non-supplied power of an outage region) but also by its frequency of occurrence. Thus, it is necessary to determine how many times each PD is expected to operate in a given time horizon. As a general rule, failure rates are given in events/km. Therefore, the number of operations of a given PD during the planning horizon depends mainly on the size of the PD's primary protection zone, which, in turn, depends on the allocation of other PDs.

An illustrative example of how the allocation of PDs affects the network's expected energy not supplied (EENS) is shown in Fig. 2. In this example, we consider the same rate of failure ( $\lambda$ ) and nodal power demand (P) for every branch and node, respectively. The hatched areas indicate the primary protection zone of each PD. It can be noticed that the area affected by the operation of  $x_1$  is the same in both cases, i.e. the entire system  $(P_{x1} = 9P)$ . However, the PD's operation frequency changes, affecting the network's total EENS, which is given by the sum of the products between the failure rates and downstream power of each protection zone. Hence, the minimum EENS would be attained by installing a PD on every branch since it would minimize the area affected by each fault event (i.e., the area downstream of the closest PD upstream of the fault). However, coordinating multiple PDs, i.e., complying with (4)-(25) can be challenging, thus leading to the optimization of the allocation taking into account the coordination constraints, which is the motivation of this paper.

In this context, creating a mathematical formulation for the optimal allocation and coordination of PDs considering any reliability-related objective function is challenging due to the fact that a PD's number of operations in the planning horizon is a variable rather than a parameter, as it depends on the allocation of other PDs, which is also a variable. To address this issue, we propose the use of four additional variables, namely  $z_i$ ,  $z_{ij}^0$ ,  $z_{ij}$ , and  $z_{ij}^{FB}$ . Variable  $z_i$  is the complementary value of  $x_i$  and indicates that there is no PD installed in branch i.  $z_{ij}^0$  represents a "clear path" between branches i and j, i.e., in order for  $z_{ij}^0$  be equal to one, there must not be a PD (except for IDs) at branches i, j, or any of the branches connecting the two.  $z_{ij}$  represents another sort of "clear path" between branches i and j. However,  $z_{ij} = 1$  only if (1) there is either a fuse or a recloser installed in branch i and (2) there

is a clear path between branches i and j. Thus, if there is neither a fuse nor a recloser in branch i, then  $z_{ij}=0$  even if there is a clear path between i and j. Finally,  $z_{ij}^{FB}$  is similar to  $z_{ij}$ , the difference being the fact that  $z_{ij}^{FB}=1$  if there is a fuse employing fuse-blow scheme installed in branch i instead of any kind of PD. The mathematical formulation of the four variables is presented in (26)–(29).

$$\chi_i + z_i = 1 \quad \forall i \in \Omega \tag{26}$$

$$z_{ij}^{0} = \left(\prod_{k \in \Omega_{i}^{d} \cap \Omega_{j}^{u}} z_{k}\right) \quad \forall i \in \Omega, j \in \Omega_{i}^{d*}$$

$$(27)$$

$$z_{ij} = \chi_i z_{ki}^0 \quad \forall i \in \Omega, j \in \Omega_i^{d*}, k \in \{\Omega_i^{d*} \cap \Omega_i^u\}$$
 (28)

$$z_{ii}^{FB} = \chi_i^{FB} z_{ki}^0 \quad \forall i \in \Omega, j \in \Omega_i^{d*}, k \in \{\Omega_i^{d*} \cap \Omega_i^u\}$$
 (29)

The nonlinear formulations shown in (27)–(29) can be re-written in a linear fashion as presented in (32)–(37).

$$z_{ij}^0 \leq z_k \quad \forall i \in \Omega, j \in \Omega_i^{d*}, k \in \Omega_i^d \cap \Omega_j^u \tag{30} \label{eq:30}$$

$$z_{ij}^{0} \ge \left( -\sum_{k \in \Omega_{i}^{d} \cap \Omega_{i}^{u}} \chi_{k} \right) + z_{i} \quad \forall i \in \Omega, j \in \Omega_{i}^{d*}$$

$$(31)$$

$$z_{ij} \le z_k \quad \forall i \in \Omega, j \in \Omega_i^{d*}, k \in \Omega_i^d \cap \Omega_i^u$$
 (32)

$$z_{ij} \le \chi_i \quad \forall i \in \Omega, j \in \Omega_i^{d*}$$
 (33)

$$z_{ij} \ge \left(-\sum_{k \in \Omega_i^d \cap \Omega_j^u} \chi_k\right) + \chi_i \quad \forall i \in \Omega, j \in \Omega_i^{d*}$$
(34)

$$z_{ij}^{FB} \le z_k \quad \forall i \in \Omega, j \in \Omega_i^{d*}, k \in \Omega_i^d \cap \Omega_i^u$$
 (35)

$$z_{ij}^{FB} \le \chi_i^{FB} \quad \forall i \in \Omega, j \in \Omega_i^{d*}$$

$$(36)$$

$$z_{ij}^{FB} \ge \left( -\sum_{k \in \Omega_i^d \cap \Omega_j^u} \chi_k \right) + \chi_i^{FB} \quad \forall i \in \Omega, j \in \Omega_i^{d*}$$
 (37)

Considering that permanent faults will cause an outage regardless of the installed PDs and temporary faults will provoke an outage only if the fault occurs inside the primary protection zone of a fuse employing fuse-blow scheme, the ECENS for permanent and temporary faults can be calculated as shown in (38) and (39), respectively. Observe that variable  $z_{ij}$  is employed to describe the PDs' primary protection zone as a function of the allocation variables in (38) and (39), i.e., a branch can be within a PD's primary protection zone only if it is downstream of such PD. As for  $z_{ij}^0$  and  $z_{ij}^{FB}$ , they are used in the next subsections.

$$e_{iwy}^{ENS} = \sum_{t \in \Phi} \phi_t P_{tiy} \left( \chi_t \lambda_{iw} + \sum_{j \in \Omega_i^{d*}} z_{ij} \lambda_{jw} \right)$$

$$\forall i \in \Omega, w = \mathcal{P}, y \in \theta \tag{38}$$

$$e_{iwy}^{ENS} = \sum_{t \in \Phi} \phi_t P_{tiy} \left( \chi_i^{FB} \lambda_{iw} + \sum_{j \in \Omega_i^{d*}} Z_{ij}^{FB} \lambda_{jw} \right)$$

$$\forall i \in \Omega, w = \mathcal{T}, y \in \theta \tag{39}$$

#### 3.4. Expected load restoration calculation

The ECENS calculated in (38) and (39) disregard the possibility of load restoration. In this subsection, we enhance such calculation by presenting the formulation for the expected energy restoration. The calculation of the expected energy restoration due to the island operation of dispatchable DGs is given by (40). Analogously, expected energy restoration due to load transferring maneuvers to neighboring feeders is given by (41). Observe that the terms between parenthesis

in (40) and (41) will increment the values of  $e_{iy}^{IO}$  and  $e_{iy}^{LT}$  only if two conditions are met. Firstly, the fault location (branch f) is not downstream of the AS. Secondly, the fault must occur within the protection zone of a PD that is upstream of the AS location, which would lead to an outage event within the islanding/transferring region. The two conditions are ensured by including  $z_{jf}$  in the product. Finally, constraints (42) and (43) ensure that the demand of the restoration areas, defined as downstream of the locations of IDs and ASs, do not surpass the capacities of the DGs and neighboring feeders contained in these areas.

$$e_{iy}^{IO} = Y_w \cdot x_i^{ID} \sum_{t \in \Phi} \phi_t P_{tiy} \left( \sum_{j \in \Omega_i^{u*}} \sum_{f \in \Omega_j^d \setminus \Omega_i^d} z_{jf} \lambda_{fw} \right)$$

$$\forall i \in \Omega, w = \mathcal{P}, y \in \theta \tag{40}$$

$$e_{iy}^{LT} = Y_w \cdot x_i^{LT} \sum_{t \in \boldsymbol{\Phi}} \phi_t P_{tiy} \left( \sum_{j \in \Omega_i^{us}} \sum_{f \in \Omega_j^d \setminus \Omega_i^d} z_{jf} \lambda_{fw} \right)$$

$$\forall i \in \Omega, w = \mathcal{P}, y \in \theta \tag{41}$$

$$x_i^{ID} \left( P_{iy} - \sum_{j \in \Omega_i^d} P_{jy}^{DG} \right) \le 0 \quad \forall i \in \Omega, y \in \theta$$
 (42)

$$x_i^{LT} \left( P_{iy} - \sum_{j \in \Omega^d} P_{jy}^{NF} \right) \le 0 \quad \forall i \in \Omega, y \in \theta$$
 (43)

Finally, the calculation of restored energy due to island operation and load transfer as shown in (40) and (41) presents nonlinear formulations due to the products  $x_i^{ID}z_{jf}$  and  $AS_i^{ILT}z_{jf}$ . Next, we present the method employed to replace the original formulation presented in (40) with the linear set of constraints (44)–(45). Nonetheless, the same process can be applied to linearize (41). It should be pointed out that if there is no ID installed in branch i, then (45) limits the maximum restoration at 0 kWh and, given that the  $e_{iy}^{IO}$  is nonnegative,  $e_{iy}^{IO}=0$ . Alternatively, if there is an ID located in branch i, (45) does not restrain  $e_{iy}^{IO}$ , while (44) sets the upper limit as the total energy demanded by nodes downstream node i. Given that the utility's objective is to maximize the restored load, the restored energy is equal to the limit imposed by (44).

$$e_{iy}^{IO} \leq Y_w \sum_{t \in \Phi} \phi_t P_{tiy} \left( \sum_{j \in \Omega_i^{u*}} \sum_{f \in \Omega_j^d \setminus \Omega_i^d} z_{jf} \lambda_{fw} \right)$$

$$\forall i \in \Omega, w = \mathcal{P}, y \in \theta \tag{44}$$

$$e_{iv}^{IO} \le M \cdot x_i^{ID} \quad \forall i \in \Omega, y \in \theta$$
 (45)

In addition to island operation and load transfer to neighboring feeders, it is possible to restore healthy out-of-service areas by isolating the faulty section via AS operation after the fault has been properly cleared by a PD with maneuvering capability (e.g., reclosers). This kind of AS maneuver allows the restoration of healthy sections downstream of the PD responsible for clearing the fault and not downstream of the AS because, once the fault is isolated by opening the AS, the upstream PD can be closed thus restoring the loads located between the PD and the AS. It should be highlighted that, in this paper, we consider an isolation maneuver to be feasible if (1) the fault is cleared by the first PD upstream of the AS, (2) the fault is downstream of the AS, and (3) only one AS operates to isolate the fault. In order to model these three constraints while ensuring the operation of the most efficient AS to isolate each fault, we introduce auxiliary variable  $z_{iif}^{AS}$ . This variable indicates that the AS located at branch j is the most adequate switch within the protection zone defined by the PD located at branch i to isolate a fault in branch f, and is calculated as shown in (46)–(50). Observe that, as per (46)–(48), the isolation maneuver can

be performed (i.e.,  $z_{ijf}^{AS}=1$ ) only if the AS and the fault are within the same protection zone (defined by the PD located at branch i) and the fault is downstream of the AS location. Constraints (49)–(50) ensure that  $z_{ijf}^{AS}$  can be equal to one only if there is a recloser at branch i and an AS at branch j. Finally, (51) prohibits the operation of more than one AS to isolate a fault.

$$z_{iif}^{AS} \le z_{ii}^{0} \quad \forall i \in \Omega, j \in \Omega_{i}^{d*}, f \in \Omega_{i}^{d*}$$

$$\tag{46}$$

$$z_{i:f}^{AS} \le z_{if}^{0} \quad \forall i \in \Omega, j \in \Omega_{i}^{d*}, f \in \Omega_{i}^{d*}$$

$$\tag{47}$$

$$z_{iif}^{AS} = 0 \quad \forall i \in \Omega, j \in \{\Omega \setminus \Omega_i^{d*}\}, f \in \{\Omega \setminus \Omega_i^{d*}\}$$
 (48)

$$z_{iif}^{AS} \le x_i^{AS} \quad \forall i \in \Omega, j \in \Omega_i^{d*}, f \in \Omega_i^{d*}$$
 (49)

$$z_{ijf}^{AS} \le \chi_i^R \quad \forall i \in \Omega, j \in \Omega_i^{d*}, f \in \Omega_j^{d*} \tag{50}$$

$$\sum_{j \in \Omega_i^d \cap \Omega_f^u} z_{ijf}^{AS} \le 1 \quad \forall i \in \Omega, f \in \Omega_i^{d*}$$

$$(51)$$

The total power that can be restored after an isolation maneuver is given by the collective power of the nodes downstream of the PD and not downstream of the AS. Nonetheless, it is possible that some of these nodes would be restored via island operation or loadtransferring maneuvers and, therefore, should not be accounted for as power restoration due to an isolation maneuver. In this context, we introduce auxiliary variable  $\rho_{ijyf}$ , calculated as shown in (52)–(54). The total restored power due to island operation and load transfer associated with the action of IDs and ASs located at branch k is calculated in (52) and (53), respectively. Next,  $\rho_{ijyf}$  is calculated as the aggregated restoration capacity due to islanding and transferring associated with the operation of devices located downstream of the PD located at branch i and not upstream of the AS located at branch k, which will be operated to permanently isolate a downstream fault. Thus, the power restoration capacity of maneuvering the AS at branch *j* to isolate downstream faults is calculated per (55). Once the restoring capacity due to maneuvering each AS to isolate downstream faults is calculated, it is possible to determine the expected energy restored by each of the ASs throughout the planning horizon, as per (56). It is important to reinforce that a single AS can be maneuvered to clear a given fault at branch f; hence, the power restoration capacity must be multiplied by the auxiliary variable  $z_{ijf}^{AS}$  which determines whether or not the AS at branch *j* should operate to isolate the fault.

$$p_{ky}^{IO} = x_k^{ID} \sum_{t \in \Phi} \phi_t P_{tky} \quad \forall k \in \Omega, y \in \theta$$
 (52)

$$p_{ky}^{LT} = x_k^{LT} \sum_{t \in \Phi} \phi_t P_{tky} \quad \forall k \in \Omega, y \in \theta$$
 (53)

$$\rho_{ijfy} = z_{ij} \sum_{k \in \{\Omega_i^{d*} \backslash \Omega_i^{d*}\}} \left( p_{ky}^{IO} + p_{ky}^{LT} \right) (1 - z_{kf}^0) z_{ijf}^{AS}$$

$$\forall i \in \Omega, j \in \Omega_i^d, f \in \Omega_j^{d*}, y \in \theta$$
 (54)

$$p_{jfy}^{IM} = \sum_{i \in \Omega_i^u} \sum_{t \in \Phi} (P_{tiy} - P_{tjy}) \phi_t z_{ij}^R - \rho_{ijfy}$$

$$\forall i \in \Omega, j \in \Omega_i^d, f \in \Omega_i^d, y \in \theta \tag{55}$$

$$e_{jy}^{IM} = \sum_{i \in \Omega_{j}^{u}} \sum_{f \in \Omega_{j}^{d}} p_{jfy}^{IM} z_{ijf}^{AS} \lambda_{fw} \quad \forall j \in \Omega, w = \mathcal{T}, y \in \theta$$
 (56)

Notably, (54) and (56) present nonlinear formulations, which can be rewritten as the sets of linear constraints shown in (57)–(59) and (60)–(62).

$$\rho_{ijfy} \geq \sum_{k \in \{\Omega_{i}^{d^*} \setminus \Omega_{j}^{d^*}\}} \left( p_{ky}^{IO} + p_{ky}^{LT} - M z_{kf} \right) - M \left( 1 - z_{ijf}^{AS} \right)$$

$$\forall i \in \Omega, j \in \Omega_i^d, y \in \theta \tag{57}$$

$$\rho_{iify} \le M \cdot z_{iif}^{AS} \quad \forall i \in \Omega, j \in \Omega_i^d, y \in \theta$$
 (58)

$$\rho_{iify} \ge 0 \quad \forall i \in \Omega, j \in \Omega_i^d, y \in \theta$$
 (59)

$$\epsilon_{jfy} \le p_{ify}^{IM} \cdot \lambda_{fw} \quad \forall j \in \Omega, f \in \Omega_j^d, w = \mathcal{T}, y \in \theta$$
 (60)

$$\epsilon_{jfy} \le \sum_{i \in \Omega_j^u} M \cdot z_{ijf}^{AS} \quad \forall j \in \Omega, f \in \Omega_j^d, y \in \theta$$
 (61)

$$e_{jy}^{IM} = \sum_{f \in \Omega_i^d} \epsilon_{jfy} \quad \forall j \in \Omega, y \in \theta$$
 (62)

Finally, the network's ECENS can be calculated as presented in (63).

$$CENS = \sum_{y \in \theta} \left[ \frac{\sum_{i \in \Omega} \sum_{w \in \Delta} e_{iwy}^{ENS} - e_{iy}^{IO} - e_{iy}^{LT} - e_{iy}^{IM}}{(1 + IRR)^y} \right]$$
(63)

#### 3.5. Problem reformulation as a MILP model

Some of the constraints shown in Section 3.2 present logical flaws. The corrections employed to obtain a feasible MILP model are addressed in this subsection.

Firstly, it should be mentioned that the coordination constraints between PDs i and j must hold true only if both are allocated. Taking (13) as an example, observe that if there is a fuse installed in branch j, but there is no recloser at branch i the problem becomes infeasible since the left-hand side would be zero and the right-hand side would not. To avoid this issue, the big-M-based relaxation shown in (64) is adopted to replace (13). The other coordination constraints, namely (12)–(16) and (25), were also replaced by their relaxed formulations using the same method.

$$\begin{aligned} x_{ic}^{RD} I_{ijc}^{rd-max} + M \left( 1 - \chi_i^R \right) &\geq \\ \kappa^{51-F} \left[ \sum_{a \in \mu^a} (x_{ja}^{FB} + x_{ja}^{FS}) T_{jjd}^{f-min} -M (1 - \chi_j^F) \right] \\ \forall i \in \Omega, j \in \Omega_i^{d*}, c \in \mu^d \end{aligned} \tag{64}$$

Observe in (64) that if there is no recloser at branch i, the left-hand side becomes a large value automatically complying with the constraint. Analogously, if there is no fuse installed in branch j, the right-hand side of (64) takes a negative value, holding true the constraint. The same conclusion is reached when there is no PD installed in either branch.

A logic flaw can be noticed in (17), which ensures that any upstream recloser must protect a fuse operating under a fuse-save scheme located at branch j in case of a temporary fault. This should not be the case when there are series reclosers, i.e., only the closest upstream recloser must operate faster than the fuse. Thus, we first introduce variable  $z_{ij}^R$ , which is analogous to  $z_{ij}^{FB}$  and is calculated in (65)–(67). This variable indicates that the only recloser between branches i and j is located at branch i. Next, we replace (17) with (68).

$$z_{ij}^{R} \le (1 - \chi_{k}^{R}) \quad \forall i \in \Omega, j \in \Omega_{i}^{d*}, k \in \Omega_{i}^{d} \cap \Omega_{i}^{u}$$
 (65)

$$z_{ii}^{R} \le \chi_{i}^{R} \quad \forall i \in \Omega, j \in \Omega_{i}^{d*}$$
 (66)

$$z_{ij}^{R} \ge \left(-\sum_{k \in \Omega_{i}^{d} \cap \Omega_{j}^{u}} \chi_{k}^{R}\right) + \chi_{i}^{R} \quad \forall i \in \Omega, j \in \Omega_{i}^{d*}$$

$$t_{i}^{RF} - M \chi_{i}^{R} \le \kappa^{50 - F} \sum_{d \in u^{a}} z_{ij}^{R} \chi_{jd}^{FS} T_{jjd}^{f - min} + M(1 - F_{i}^{S})$$

$$(67)$$

$$\forall i \in \Omega, j \in \Omega_i^{d*} \tag{68}$$

It should be mentioned that (68) is nonlinear due to the product  $z_{ij}^R x_{jd}^{FS}$ . Thus, (68) is rewritten as (69).

$$\begin{aligned} t_i^{RF} - M \chi_i^R - M (1 - z_{ij}^R) &\leq \kappa^{50 - F} \sum_{d \in \mu^a} z_{ij}^R \chi_{jd}^{FS} T_{jjd}^{f - min} \\ &+ M (1 - \chi_i^{FS}) + M (1 - z_{ij}^R) \quad \forall i \in \Omega, j \in \Omega_i^{d*} \end{aligned}$$
(69)

For completeness' sake, the resulting MILP formulation proposed in this paper is shown in (70)–(71).

$$min \{Investment Costs + CENS:(1)+(63)\}$$
 (70)

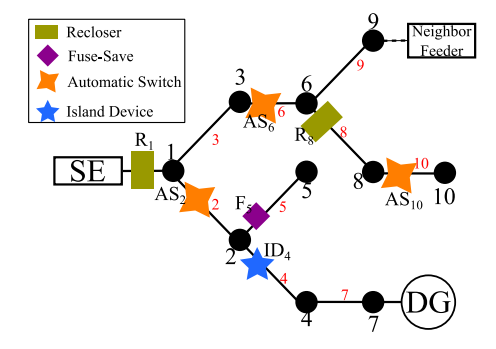


Fig. 3. Protection system topology for the illustrative example.

It should be mentioned that some sets of constrains listed in (71), namely (11)–(16), (17), (27)–(29), (40)–(41), (54), and (55), present nonlinear formulations. Nonetheless, the methods used to linearize each of them are shown in (64), (65)–(68), (30)–(37), (44)–(45), (57)–(59), and (60)–(62), respectively.

#### 3.6. Illustrative example

In this subsection, we present an instructive example regarding the set of constraints presented in (71). Admittedly, the optimization problem presented in (70)–(71) was not solved to attain the optimal sitting and sizing of PDs and CDs for this study since, instead we have considered the protection system topology (i.e., location of PDs and CDs) as input and evaluate how the set of constraints presented in (71) work. Evidently, a different topology may be better cost-wise; however, any solution that does not comply with the logic discussed in this example is infeasible. For the sake of simplicity, the year index is omitted from this example.

For this example, consider a DS with the topology and allocation of PDs (i.e.,  $R_1$ ,  $ID_4$ ,  $F_5$ , and  $R_8$ ) and CDs (i.e.,  $AS_2$ ,  $AS_6$ , and  $AS_{10}$ ) illustrated in Fig. 3. Firstly, (13) indicates that the delayed operation of  $R_1$  (represented at the left-hand side of (13)) takes longer than the time needed to melt  $F_5$  (represented at the right-hand side of (13)), which indicates the coordination of these PDs under a scenario of permanent fault at branch 5. For a temporary fault, (17) guarantees that the recloser operates first, since  $t_i^{RF}$ , representing the recloser's action time under fast operation at the left-hand side of (17), must be less than the fuse's minimum melting time, represented by  $x_{ja}^{FS}T_{jja}^{f-min}$  at the right-hand side of (17). As a result, the load downstream of  $F_5$  does not suffer an outage if there is a temporary fault at branch 5, as the recloser operates first and once the reclosing maneuver is performed the fault is no longer in the DS and every load is resupplied.

Similarly, constraints (12) and (15) ensure that  $R_1$ , represented in the left-hand side in both constraints, must take longer to act than  $R_8$ , indicating a selective operation for permanent and temporary faults downstream of  $R_8$ . If there were any other PD that demands coordination downstream of  $R_1$ , the correspondent constraint would ensure proper coordination; noteworthy, despite being a PD,  $ID_4$  does not require coordination with any PD as this device operates for upstream faults while every other PD operates for downstream faults. Observe that, even though constraints (14) and (16) are not addressed in this example, they are formulated and handled exactly as (12), (13), and (15), in the sense that the backup PD, represented at the left-hand side, must always take longer to operate than the primary PD, represented at the right-hand side of the constraints.

Next, we address how EENS and energy restored are calculated. As per (38)-(39), the EENS associated with the operation of each recloser and fuse allocated in the DS is calculated. Since there is no fuse adopting fuse-blow scheme in this DS, (39) is disregarded as no load will experience an outage due to temporary faults, as explained in Section 2.1: nonetheless, it should be mentioned that the same analysis presented for (38) can be extended for (39). Observe in (38) that if there is no recloser nor fuse at branch i, then  $e_{iw}^{ENS} = 0$  since  $x_i =$  $z_{ii} = 0$ . Thus, the EENS can be calculated only for branches 1, 5, and 8. The second term of (38) accounts for the failure rate of every branch j downstream of i as long as there are no PD between branches i and j (guaranteed by  $z_{ij}$ ). In this sense, the number of operations expected for R<sub>1</sub> is given by the sum of the failure rates of the branches within its primary protection zone, i.e., every branch downstream of  $R_1$  and not downstream of any other PD (i.e.,  $\lambda_{1\mathcal{P}}+\lambda_{2\mathcal{P}}+\lambda_{3\mathcal{P}}+\lambda_{4\mathcal{P}}+$  $\lambda_{6P} + \lambda_{7P} + \lambda_{9P}$ ). Accordingly, F<sub>5</sub> is expected to operate at the same number of expected failures as branch 5 (i.e.,  $\lambda_{5P}$ ), and  $R_8$  should operate for faults in branches 8 and 10 (i.e.,  $\lambda_{8P} + \lambda_{10P}$ ). The power curtailed by the operation of R<sub>1</sub>, disregarding restoration possibilities, is the total demand of the DS (i.e.,  $P_1$ ), while the outage power due to the operation of  $F_5$  and  $R_8$  is equal to the demand at node 5 and 8, respectively (i.e.,  $P_5$  and  $P_8$ ).

Regarding load restoration via island operation and load transferring, (42)–(43) guarantee that an ID and a AS for load transference can be allocated only if the generator and neighboring feeder, respectively, have enough capacity to supply the additional load. In this sense,  $AS_2$  and  $AS_{10}$ , which have no downstream neighboring feeder, cannot perform load transfers. Moreover, the load downstream of  $ID_4$  must not surpass the capacity of the DG; the same applies for the demand downstream of  $AS_6$  and the capacity of the neighboring feeder. Granting these assumptions, the analysis continues as follows.

The term between parenthesis in (40)-(41) indicates that the power downstream of the ID or AS is restored for every fault that occurs within the protection zone of a PD located upstream of the ID or AS. It is important to highlight that the simple fact that a fault is not downstream of an ID or AS is not enough to cause load restoration via island operation or load transfer to neighboring feeders. If the PD responsible for clearing the fault is not upstream of the ID or AS, then the clearing process does not cause an outage within the islanding/transferring regions, and such restoration is not necessary. Observe, in Fig. 3, that a fault at branch 5 is not downstream of ID<sub>4</sub> or AS<sub>6</sub> and yet clearing it does not provoke an outage in the islanding and load transferring regions as the operation of F<sub>5</sub> does not affect such parts of the DS. Analogously, the operation of R<sub>8</sub> to clear a fault either in branch 8 or 10 does not lead to an outage in the region downstream of ID<sub>4</sub>. Thus, the expected number of operations for ID<sub>4</sub>, as per (40), is given by  $\lambda_{1P} + \lambda_{2P} + \lambda_{3P} + \lambda_{6P} + \lambda_{9P}$ , while the restored power is given by the total demand downstream of  $ID_4$  (i.e.,  $P_4$ ). As for  $AS_6$ , the expected number of operations is given by  $\lambda_{1P} + \lambda_{2P} + \lambda_{3P} + \lambda_{4P} + \lambda_{7P}$ , as per (41), and each operation restores the total demand downstream of  $AS_6$  (i.e.,  $P_6$ ). Observe that branches 6, 8, 9 and 10 are within the load transferring region and therefore the load will not be transferred if the fault is downstream of node 3. Finally, since the restoration capacity of AS2 and AS8 is zero, it is not possible to allocate an AS with load transferring purposes (i.e.,  $x^{LT}$ ) at these branches, as per (43).

Load restoration via isolation maneuver is the most complex formulation amongst the ones considered in this paper since the restored power is not simply given by the total demand downstream of the maneuvered AS, but by the sum of demands of the loads comprised in the area between the AS and the first upstream PD, which is responsible for clearing the fault. For example, considering a fault at branch 9 of the DS shown in Fig. 3,  $R_1$  is responsible for clearing the fault and  $AS_6$  is used to permanently isolate the fault so that  $R_1$  can be reclosed, restoring loads at nodes 1, 2, 3, and 5 (observe that the loads at nodes 4 and 7 are restored via island operation; furthermore,

load transferring is not possible since the fault is within the transferring region). Remarkably, once the fault is permanently isolated, the island can be re-synchronized with the main grid. However, from an EENS perspective, both operating scenarios are the same since the loads are fully supplied in both cases. Thus, we do not address the resynchronization process in this paper.

Alternatively, if the fault occurs at branch 7, then AS<sub>2</sub> is responsible for permanently isolating the fault after the operation of R<sub>1</sub> (since an ID operates only for faults upstream of the islanding region), leading to the restoration of node 3 only, given that nodes 6, 8, 9, and 10 would be restored via load transfer regardless of the fault isolation maneuver performed by AS<sub>2</sub>. Again, once the fault has been permanently isolated, nodes 6, 8, 9, and 10 can be reconnected into the main grid; however, such maneuver is disregarded in this paper as the EENS remains unchanged. As can be noticed in these examples, load restoration via fault isolation depends on both fault location and protection system topology. As a final example of IM, consider a fault in branch 10. Then, R<sub>8</sub> is responsible for clearing the fault, leading to an outage in nodes 8 and 10. After the fault has been cleared, AS<sub>10</sub> must operate to permanently isolate the fault followed by the reclosing maneuver of R<sub>8</sub> which restores the load in node 8. However, if coordination constraints are not regarded then R<sub>1</sub> may operate faster than R<sub>8</sub> and, in this context, the outage region would be much greater leading to unexpected costs and continuity indices. Thus, the proposed formulation provides more reliable results since the outage area calculated by in this approach does not increase due to the lack of selectivity as opposed to that of [12,13].

In the proposed formulation,  $\rho_{ijf}$ , calculated in (57)–(59), represents the power that would be restored regardless of the fault isolation maneuver either by island operation or load transfer, and thus should not be accounted for as load restored due to fault isolation maneuver. Considering the topology presented in Fig. 3,  $\rho_{ijf}$  would be bounded only by (59) for every  $i \neq \{1,8\}$  since the right-hand side of (57) would be negative due to the term  $-M(1-z_{ij}^{AS})$ .

be negative due to the term  $-M(1-z_{iff}^{AS})$ . Additionally,  $\rho_{ijf}$  depends on the location of the AS, i.e., branch j as well as on the location of the fault f. Taking for example AS<sub>2</sub>, we have  $\rho_{12f} \geq p_6^{LT} + p_4^{IO} \ \forall f \in \{2,5\}$ , and  $\rho_{12f} \geq p_6^{LT} \ \forall f \in \{4,7\}$ , as per (57) since in the first case  $z_{4f} = z_{6f} = 0$  and, in the second  $z_{4f} = 1$  and  $z_{6f} = 0$ . This means the island cannot be performed for the second case because the fault is within the islanding region and, therefore, should not be accounted for as restored power. Analogously,  $\rho_{16f} \geq p_4^{IO} \ \forall f \in \{6,8,9\}$ . Observe that, although AS<sub>6</sub> could operate to permanently isolate a fault located in branch 10, it would not be the best choice to restore power. Thus,  $z_{16,10}^{AS} = 0$  and so is  $\rho_{16,10}$  and  $\rho_{16,10}^{IM}$ . Finally,  $\rho_{8,10f} \geq p_4^{IO} \ \forall f \in \{10\}$ , observe that  $\rho_6^{LT}$  is not considered as the fault is within the transferring region and therefore  $z_{6f} = 1$  in (57). It is important to stress that  $\rho_{ijf}$  is a nonnegative variable. Therefore, the higher the value of  $\rho_{ijf}$ , the lower the energy restoration via fault isolation maneuvers, as per (56), which, in turn, worsens the objective function. Thus, the inequalities regarding  $\rho_{ijf}$  presented in this paragraph are always binding, i.e., the equality always holds true either for (57) or (59).

As for  $p_{jf}^{IM}$ , it is given by the difference between the power downstream of branch i, wherein the PD and is upstream of the AS location j, and the power downstream of branch j (i.e.,  $P_{iiy}-P_{tjy}$  in (55)) minus the power restored by island operation and load transfer due to the operation of any element located at branches downstream of j (i.e.,  $\rho_{ijf}$  in (55)) considering a fault at branch f.

The expected energy restoration due to isolation maneuvers depends not only on the power restoration, calculated in (55), but also on how many times such maneuver is expected to happen, which is given by (56). Observe that  $e_{jy}^{IM}$  equals the power restoration limit  $(p_{jf}^{IM})$  times the expected number of faults for branch  $f(\lambda_{fP})$  only if  $z_{ijf}^{AS}=1$ , i.e., the energy is restored only if the AS located at branch j is the most efficient switch to be used for the isolation of a fault at branch f after it has been cleared by the PD located at branch i. Noteworthy, there can be only one switch maneuver to isolate a fault as per (51). In

this sense, the most efficient switch to be operated to isolate a fault is the closest AS upstream of the fault location.

Thus, AS<sub>2</sub> should operate to permanently isolate faults at branches 2, 4, and 7 after R<sub>1</sub> clears these faults, for example. Observe that node 5 is not included, as the fault is cleared by F<sub>5</sub>, which is not upstream of AS<sub>2</sub>, such effect is guaranteed in (56) since  $z_{125}^{AS}=0$  due to (47) given that  $z_{25}^0=0$ . Similarly, the other branches also cause  $z_{12f}^{AS}=0$  as  $i\neq 1$  is not upstream of branch 2. Hence, the total energy restored by maneuvering AS<sub>2</sub> for fault isolation is given by  $e_2^{IM}=p_{2f}^{IM}\cdot z_{12f}^{AS}\cdot \lambda_{fP}$   $\forall f\in\{2,4,7\}$ , as per (56). By expanding this expression using (55), it is possible to rewrite the total energy restoration as  $e_2^{IM}=(P_1-P_2)-(p_6^{LT}+p_4^{IO})\cdot (\lambda_{2P})-(p_6^{LT})\cdot (\lambda_{4P}+\lambda_{7P})$ .

#### 4. Results

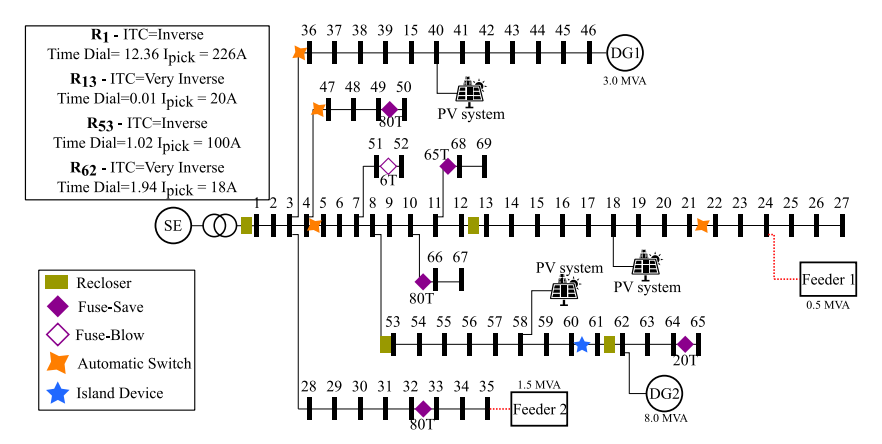
The proposed model was validated for a 69-node distribution system considering a 5-year planning horizon. Data regarding the power system, coordination factors, and cost-related parameters can be found in [30]. All case studies were solved using Gurobi 11.0.0 [31] under AMPL [32]. In this paper, we set the reclosers' minimum tripping time (i.e.,  $\underline{R}'$ ) as 0. The maximum and minimum short-circuit currents (SCCs) were obtained by applying solid three-phase and single- and two-phase 30  $\Omega$  faults, respectively, at the end terminal of every branch. The fault study was carried out considering a single pre-fault condition. The use of a probabilistic short-circuit study instead of a deterministic one has been show to be useful [22,24]. However, the goal of this article is to present a MILP formulation for the optimization problem rather than highlighting the benefits of employing a probabilistic short-circuit study.

This section is divided into two subsections. The first presents an economic evaluation of the proposed model featuring direct comparisons between the proposed method and other approaches found in the literature. In the second subsection, we discuss the optimal protection topology and the coordination/selectivity feasibility that supports the economic prospects, which cannot be validated for other formulations that address cost-effectiveness maximization while disregarding coordination constraints.

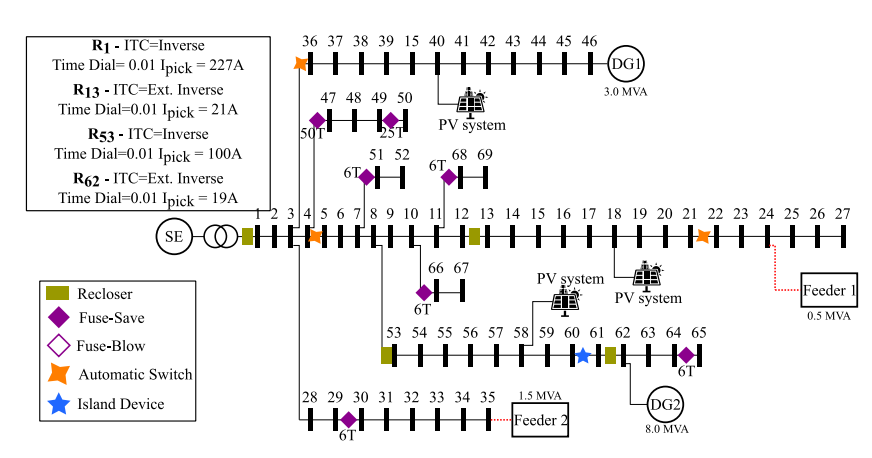
#### 4.1. Validation of the proposed model

The advantages of the proposed method are highlighted by confronting its cost-effectiveness against intermediate models, which are partially featured in articles published in the specific literature. Six case studies are considered; case 1 disregards every possibility of load restoration. Every paper mentioned in Table 1 considers at least one restoration possibility; nonetheless, case 1 can be used as a benchmark to assess the effectiveness of the restoration possibilities; for case 2, IM is the only restoration method considered, as proposed in [7]; for case 3, LT and IM are the load restoration possibilities, as per [5,6,8]; IO and LT are considered in the most recent articles [21–24] and are featured in case 4; case 5 addresses a scenario wherein IM and IO are the only restoration methods as proposed in [10,11]; finally, the proposed method is represented in case 6, which simultaneously considers IO, LT, and IM.

It should be stressed that none of the existing approaches cited in the previous paragraph can guarantee the optimality of the solution either due to the solving technique employed or to the lack of coordination constraints to ensure operational feasibility. Furthermore, some of them, namely approaches [5,6,21], and [22], do not consider the possibility of employing the fuse-blow scheme, which is featured in the six study cases presented in this section and has been shown to produce better results [24]. Thus, case studies 1–5 already present significant gains over the original approaches as the case studies presented in this section were modeled as MILP problems and considering coordination constraints, hence ensuring optimal allocation and coordination. The



(a) Optimal protection system topology – Case 6.



(b) Optimal protection system topology – Case 7.

Fig. 4. Protection system topologies obtained for cases 6 and 7.

Table 2 Expected costs for the planning horizon (\$10<sup>3</sup>).

	ECENS	Investment cost	Total expected cost
Case 1	639.1752	135.7941	774.9693
Case 2	600.6799	114.5846	715.2645
Case 3	591.1081	120.4757	711.5838
Case 4	268.0802	141.3306	409.4108
Case 5	272.8182	131.7668	404.5850
Case 6	262.8485	137.6579	400.5064

costs associated with the optimal protection system topology obtained for each case study are presented in Table 2.

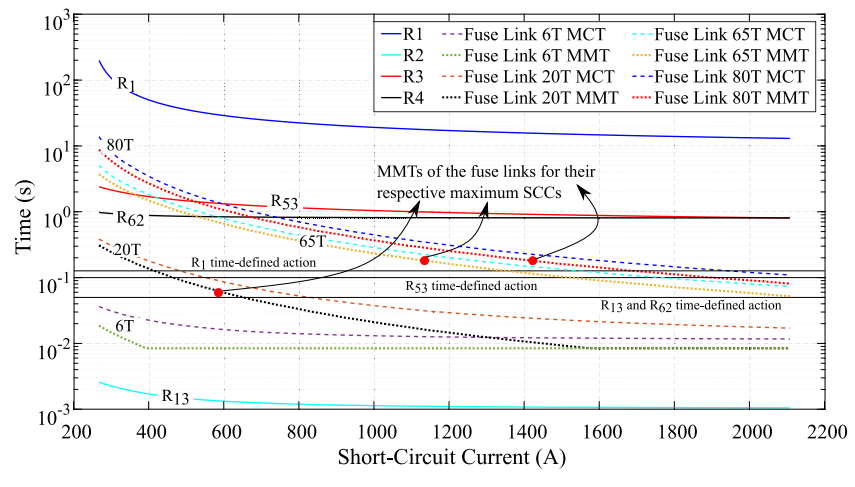
As expected, the results support the claim that increasing the number of load restoration possibilities leads to more cost-effective topologies. The cost reductions obtained for cases 2, 3, 4, 5, and 6 relative to case 1 are, respectively, 7.70%, 8.18%, 47.17%, 47.79%, and 48.32%. Hence, for this DS, the consideration of load restoration through IO is the most efficient method for this DS since the cost reduction due to LT and IM alone (i.e., case (3) is less than 10%. In contrast, the combination of IO with any other restoration possibility leads to a 47.17% cost reduction at least (i.e., case (4). Naturally, the effectiveness of each restoration method depends on the DS's characteristics, such as load density and load transferring and DG capacities, as well as on economic parameters like equipment costs and energy not-supplied costs. In summary, the effectiveness of each restoration method is expected to change for each feeder. Therefore, the only way to ensure that the more suited restoration method is applied for a specific feeder is by

considering all of them in the optimization formulation, as proposed in this paper.

#### 4.2. Technical assessment of the proposed solution

In the previous section, we have shown that the consideration of more restoration possibilities leads to more cost-effective solutions; thus, proving the advantages of the proposed formulation over those shown in [5–11,21–24]. Nonetheless, the formulations presented in [12,13] simultaneously account for IO, LT, and IM. However, coordination constraints are not regarded in these papers; therefore, we present a direct comparison between the formulation presented in Section 3 and those presented in [12,13] to highlight the differences and attest the superiority of our proposal over the remaining existing ones. To meet this end, we solved a seventh case study formulated just like case study 6 except for the exclusion of (12)– (17). The optimal allocation and setting of PDs and CDs obtained for cases 6 and 7 is illustrated in Fig. 4.

Firstly, it is possible to observe comparing Figs. 4(a) and 4(b) that the solution to case 7 presents more PDs than that obtained for case 6. As a result, the area affected by most outages, considering case 7's protection topology, should be smaller than that observed for the same fault under the protection topology obtained for case 6. Furthermore, since no fuse link employs the fuse-blow scheme, the topology shown in Fig. 4(b) should not be affected by any temporary fault. In light of these facts, the expected energy not supplied associated with case 7



### (a) Coordinogram for Case 6.

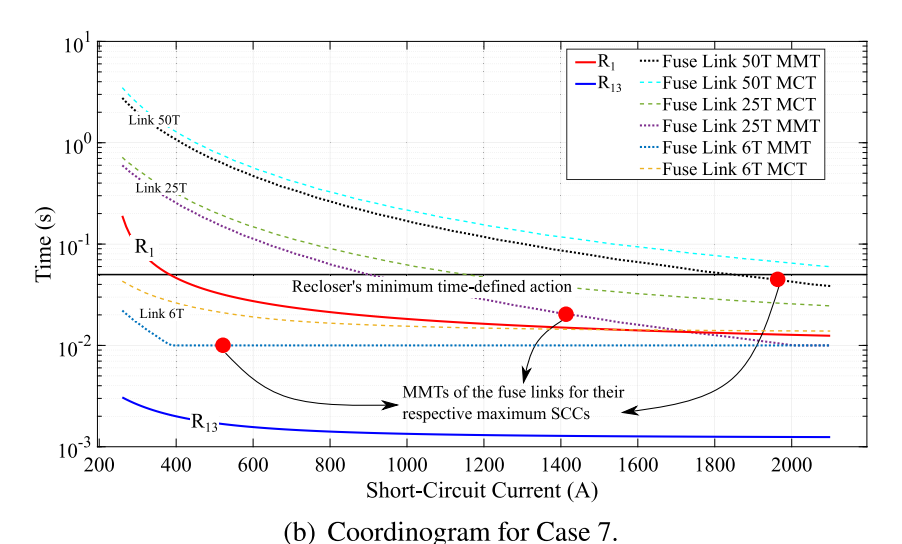


Fig. 5. Coordinograms of the protection systems obtained for cases 6 and 7.

Table 3
Total costs associated with cases 6 and 7 (\$10<sup>3</sup>).

		ECENS	Investment cost	Total cost
Case 6		262.8485	137.6579	400.5064
Case 7	Expected Actual	248.1196 320.1937	130.5941 109.6935	378.7137 429.8872

should be lower than that of case 6, as shown in Table 3 under Case 7 Expected.

Evidently, the ECENS associated with each study case will differ in real-world operation if the protection system fails to operate in a coordinated or selective manner. For example, if a recloser fails to operate before an immediately downstream fuse (employing the fuse-save scheme) melts, then the area downstream of the fuse will experience an outage not foreseen during the planning phase and, therefore, not accounted for in Table 3. Thus, if the protection system fails to coordinate, there will be larger outage areas than needed to clear a fault (and accounted for during the planning phase), increasing the ECENS. In this context, we illustrate the coordinograms of both case 6 and case 7 protection systems topologies in Fig. 5 to assess the operation of every PD in the DS.

Fig. 5(a) depicts the ITC of each recloser, as well the minimum melting time (MMT) of the fuse links located at branches 50 (80T link), 65 (20T link), and 68 (65T link) since these PDs adopt the fuse-save scheme and present the highest SCCs which hinders the coordination between fuse and recloser. It is important to mention that the timedefined operation (i.e., fast operation) of R<sub>1</sub>, illustrated in Fig. 5(a), is faster than the MMTs of  $F_{50}$  and  $F_{68}$  (consequently faster than  $F_{33}$ and F<sub>66</sub>, whose critical SCCs present lower values than that of F<sub>50</sub>). It is worth mentioning that  $F_{65}$  must coordinate with  $R_{62}$ ; therefore, the fact that its MMT is lower than the time-defined action of  $R_1$  is not a problem. Furthermore, it is possible to observe that the fuses' maximum clearing times (MCTs) values are much lower than those of the reclosers' delayed operation, i.e., fuse links 80T and 65T (F<sub>50</sub>, and F<sub>68</sub>) melt faster than the delayed operation of R<sub>1</sub> and the fuse link 20T ( $F_{65}$ ) melts faster than the delayed operation of  $R_{62}$ . In this sense, every fuse operates before their backup PD, thus minimizing the outage area when clearing permanent faults. Moreover, since there is no PD downstream of R<sub>13</sub>, the recloser operates much faster than any other device. Regarding the operation of the fuse employing the fuse-blow scheme (branch 52), it is possible to observe in Fig. 5(a) that the fuse's MMT and MCT are entirely below the time-defined action of R<sub>1</sub> (i.e., first upstream recloser). The selectivity between the recloser and the fuse is maintained since, as shown in this analysis, the recloser operates after a fuse link 80T under delayed operation. Finally, it can be observed that both delayed and fast operations of  $R_1$  take longer than those of  $R_{13}$ ,  $R_{53}$ , and  $R_{62}$ ; furthermore,  $R_{62}$  operates faster than  $R_{53}$  for the range of SCCs calculated for the DS, thus guaranteeing the selective operation among the digital PDs. For the sake of reproducibility, complete information regarding the settings of the PDs shown in Fig. 4(a) is available in Appendix.

Contrarily, the coordinogram presented in Fig. 5(b) demonstrates that the MMT of any fuse is faster than the recloser's minimum time-defined action and, therefore, cannot employ fuse-save scheme. As a result, the DS becomes vulnerable to temporary faults that will be able to cause permanent outages due to the fuse melting before the recloser's fast action. The operation of reclosers  $R_{53}$  and  $R_{62}$  is not represented in Fig. 5(b) since these devices will operate faster than  $R_1$  and  $R_{13}$  (already represented in the figure) given their settings (shown in Fig. 4(b)). Moreover, reclosers  $R_{13}$  and  $R_{62}$  operate under delayed action faster than any fuse, which characterizes a loss of selectivity. Recloser  $R_1$  also operates faster than most fuses under delayed action. The selectivity issue leads to the increase of the outage area needed to clear a fault, as the backup PD acts before the primary device.

The analysis of Fig. 5(b) leads to the conclusion that the expected costs associated with case 7 are underestimated due to the loss of coordination and selectivity. Nonetheless, one can argue that resizing the fuse links can still lead to coordination and selectivity between fuses and reclosers. Hence, we have resolved case 6 while considering only the possibility of removing and resizing the PDs allocated for case 7, thus attaining the most cost-effective way to ensure coordination of the PDs presented in Fig. 4(b). The costs associated with this new solution (obtained by removing  $R_{62}$ ,  $F_{47}$ , and  $F_{65}$  as well as resizing the other fuses and resetting the reclosers' parameters) are reported in Table 3 as Case 7 Actual. Noteworthy, every fuse in the protection system still employs the fuse-save scheme. As can be observed, the cost-effectiveness is worse (7.34%) than that attained when case 6 is directly solved.

Finally, it should be highlighted that although optimizing continuity indices such as SAIDI is not within the scope of this paper, one can safely assume that it tends to be proportional to the ECENS as per [22, 24]. Therefore, the increase in ECENS observed when comparing the expected and actual values for the case 7 solution could also lead to continuity index violation, which may not be restored since the removal of PDs causes outage areas to increase. Furthermore, depending on the feeder's and equipment parameters, some fuses can no longer operate under the fuse-save scheme, which also worsens continuity indices.

#### 5. Conclusion

This paper addresses the critical challenges in optimizing PDs and CDs allocation in DSs, emphasizing the necessity of coordination for reliable and efficient operation. Existing literature reveals a gap where approaches often consider device allocation without ensuring coordination, leading to infeasible solutions. Fewer approaches tackle the allocation and coordination problems simultaneously. Unfortunately, such proposals employ metaheuristics to solve the resulting optimization problem, which leads to suboptimal solutions.

Our contribution lies in a novel MILP formulation that integrates both device allocation (reclosers, fuses, IDs, ASs) and coordination constraints. Thus, unlike previous heuristic-based methods, our approach guarantees not only solution feasibility but also finite convergence to optimality. Moreover, island operation, feeder load transfer, and fault isolation using ASs are considered to enhance the cost-effectiveness of the protection system. This comprehensive framework was tested for a 69-node DS, and the results attest to the importance of considering multiple sources of load restoration (from an economic perspective) and the efficiency of the designed protection system (from a technical perspective). Thus, the proposed formulation provides distribution

companies with a robust tool for optimizing the design of protection systems.

Future research may address (1) the formulation of a multi-stage protection system planning in which CDs and PDs can be allocated and removed throughout the planning horizon to adapt to new operational realities, (2) the consideration of reliability indexes either in the objective function or in additional constraints, and (3) the inclusion of uncertainties due to load oscillation and intermittent power injection from renewable-based generators, which would lead to new challenges regarding the estimation of power restoration and islanding feasibility.

#### CRediT authorship contribution statement

Wandry Rodrigues Faria: Writing – original draft, Software, Methodology, Conceptualization. Gregorio Muñoz-Delgado: Writing – review & editing, Supervision. Javier Contreras: Writing – review & editing, Supervision. Benvindo Rodrigues Pereira: Writing – review & editing, Supervision.

#### **Declaration of competing interest**

The authors declare that they have no known competing financial interests or personal relationships that could have appeared to influence the work reported in this paper.

#### Acknowledgments

The work of W. R. Faria and B. R. Pereira Jr. was supported by the Coordination for the Improvement of Higher Education Personnel (CAPES) under finance code 001, the Brazilian National Council for Scientific and Technological Development (CNPq) under Grant 408464/2023-2, and the São Paulo Research Foundation (FAPESP) under Grant 2021/04628-0. The work of G. Muñoz-Delgado and J. Contreras was supported in part by the EU Horizon Europe Programme under GA ID: 101160614 (EU-DREAM Project, DOI: 10.3030/101160614) and MSCA DN GA ID: 101168796 (FITNESS Project, DOI: 10.3030/101168796), in part by Grant PID2021-122579OBI00 funded by the Spanish Ministry of Science and Innovation MCIN/AEI/10.13039/501100011033 and by "ERDF A way of making Europe", in part by Grant SBPLY/21/180501/000154 funded by the Junta de Comunidades de Castilla-La Mancha, by the Spanish Ministry of Finance and Civil Service, by European Union Funds, and by the ERDF, and in part by grant 2023-GRIN-34074, funded by the Universidad de Castilla-La Mancha, under the UCLM Research Group Program, and by the European Commission, under the ERDF.

#### Appendix. Protective devices' settings

Details regarding the optimal parameters and the coordination between the PDs are provided in Tables 4 and 5. Just as shown in Fig. 5(a), one can observe in Table 4 that R1 takes much longer than any other PD to operate. This is due to the coordination constraints that state that the backup PD when subjected to the most critical SCC shall not operate faster than the primary PD subjected to the least severe SCC. Considering the case of R1, note that F66 takes 18.95s to clear the least severe SCC within its protection zone; thus, R1 must delay more than 18.95s to clear the most severe fault within the protection zone of F66. Such restraint reflects in even greater delays to clear other faults that causes lower SCCs, for example, those downstream of R13. Although R1 presents the most critical consequences of the coordination constraints, the same analysis can be conducted for every other PD that acts as backup for another PD.

 Table 4

 Assessment of the coordination between the allocated protective devices.

Primary PD Backup PD		D Backup PD Max SCC				Min SCC				
		Primary PD Backup P.		Backup PD	kup PD		Primary PD		Backup PD	
		Current magnitude (A)	Acting time (s) <sup>a</sup>	Current magnitude (A)	Acting time (s)	Current magnitude (A)	Acting time (s) <sup>a</sup>	Current magnitude (A)	Acting time (s)	
R13	R1	957.65	0.01	1048.79	22.15	201.93	0.01	358.33	70.46	
F33	R1	1335.56	0.24	1436.73	18.62	227.59	16.28	399.24	57.34	
F50	R1	1415.02	0.21	1498.22	18.24	288.47	10.22	440.08	49.17	
F52	R1	1489.06	0.01	1559.40	17.89	261.62	0.04	429.00	51.07	
R53	R1	1552.94	1.07	1595.17	17.70	274.08	2.67	370.98	65.63	
R62	R53	740.34	0.98	746.28	1.42	213.60	1.22	266.18	2.80	
F65	R62	578.18	0.07	579.80	0.99	196.21	0.79	205.54	1.25	
F66	R1	1292.16	0.26	1367.81	19.09	253.01	18.95	418.22	53.12	
F68	R1	1127.16	0.21	1213.27	20.35	244.46	7.67	410.46	54.75	

<sup>&</sup>lt;sup>a</sup> The fuses' acting times were calculated considering the maximum clearing time curve for the minimum SCC and considering the minimum melting time curve for the maximum SCC.

**Table 5**Protective devices' sizing and parameters

(s) PC  226 A  226 A  21 A  21 A
226 A 21 A
21 A
21 A
100 A
100 A
18 A
18 A
_
_
-
_
_
_

Note: PF — Protective Function; TD — Time Dial; MCT — Maximum Clearing Time (calculated for the least severe short-circuit current within the primary protection zone); MMT — Minimum Melting Time (calculated for the most severe short-circuit current within the primary protection zone); PC — Pickup Current; I — Inverse; VI — Very Inverse: EI — Extremely Inverse.

#### Data availability

Data will be made available on request.

#### References

- [1] Jen-Hao Teng, Yi-Hwa Liu, A novel ACS-based optimum switch relocation method, IEEE Trans. Power Syst. (ISSN: 0885-8950) 18 (1) (2003) 113–120, http://dx.doi.org/10.1109/TPWRS.2002.807038.
- [2] F. Soudi, K. Tomsovic, Optimized distribution protection using binary programming, IEEE Trans. Power Deliv. (ISSN: 0885-8977) 13 (1) (1998) 218–224, http://dx.doi.org/10.1109/61.660881.
- [3] Kerry D. McBee, Izar Fareez, Chris Pardington, Identifying DA allocation by minimizing the overall cost of customer minutes interrupted, IEEE Trans. Power Deliv. 36 (3) (2021) 1694–1704, http://dx.doi.org/10.1109/TPWRD.2020.3013233.
- [4] Mohammad Farajollahi, Mahmud Fotuhi-Firuzabad, Amir Safdarian, Optimal placement of sectionalizing switch considering switch malfunction probability, IEEE Trans. Smart Grid 10 (1) (2019) 403–413, http://dx.doi.org/10.1109/TSG. 2017.2741424
- [5] A. Heidari, V.G. Agelidis, M. Kia, J. Pou, J. Aghaei, M. Shafie-Khah, J.P.S. Catalão, Reliability optimization of automated distribution networks with probability customer interruption cost model in the presence of DG units, IEEE Trans.

- Smart Grid (ISSN: 1949-3053) 8 (1) (2017) 305–315, http://dx.doi.org/10.1109/TSG.2016.2609681.
- [6] A. Heidari, Z.Y. Dong, D. Zhang, P. Siano, J. Aghaei, Mixed-integer nonlinear programming formulation for distribution networks reliability optimization, IEEE Trans. Ind. Inf. (ISSN: 1551-3203) 14 (5) (2018) 1952–1961, http://dx.doi.org/ 10.1109/TII.2017.2773572.
- [7] A. Alam, M.N. Alam, V. Pant, B. Das, Placement of protective devices in distribution system considering uncertainties in loads, temporary and permanent failure rates and repair rates, IET Gener. Transm. Distrib. (ISSN: 1751-8695) 12 (7) (2018) 1474–1485, http://dx.doi.org/10.1049/iet-gtd.2017.0075.
- [8] M. Izadi, A. Safdarian, M. Moeini-Aghtaie, M. Lehtonen, Optimal placement of protective and controlling devices in electric power distribution systems: A MIP model, IEEE Access 7 (2019) 122827–122837, http://dx.doi.org/10.1109/ ACCESS.2019.2938193.
- [9] Miguel Monteiro Costa, Michel Bessani, Lucas S. Batista, A multiobjective and multicriteria approach for optimal placement of protective devices and switches in distribution networks, IEEE Trans. Power Deliv. 37 (4) (2022) 2978–2985, http://dx.doi.org/10.1109/TPWRD.2021.3120968.
- [10] Afroz Alam, Vinay Pant, Biswarup Das, Optimal placement of protective devices and switches in a radial distribution system with distributed generation, IET Gener. Transm. Distrib. (ISSN: 1751-8687) 14 (2020) 4847–4858.
- [11] Hassan Karimi, Taher Niknam, Moslem Dehghani, Mohammad Ghiasi, Mina Ghasemigarpachi, Sanjeevikumar Padmanaban, Sajad Tabatabaee, Hamdulah Aliev, Automated distribution networks reliability optimization in the presence of DG units considering probability customer interruption: A practical case study, IEEE Access 9 (2021) 98490–98505, http://dx.doi.org/10.1109/ACCESS.2021. 3096128
- [12] Cleberton Reiz, Tayenne Dias De Lima, Jonatas Boas Leite, Mohammad Sadegh Javadi, Clara Sofia Gouveia, A multiobjective approach for the optimal placement of protection and control devices in distribution networks with microgrids, IEEE Access 10 (2022) 41776–41788, http://dx.doi.org/10.1109/ACCESS.2022. 3166918.
- [13] M. Lwin, J. Guo, N. Dimitrov, S. Santoso, Protective device and switch allocation for reliability optimization with distributed generators, IEEE Trans. Sustain. Energy (ISSN: 1949-3029) 10 (1) (2019) 449–458, http://dx.doi.org/10.1109/ TSTE.2018.2850805.
- [14] Annu Dagar, Pankaj Gupta, Vandana Niranjan, Microgrid protection: A comprehensive review, Renew. Sustain. Energy Rev. (ISSN: 1364-0321) 149 (2021) 111401
- [15] Hadi Bisheh, Bahador Fani, Ghazanfar Shahgholian, Iman Sadeghkhani, Fuse saving coordination scheme for active distribution systems: State-of-the-art and a novel quasi-voltage current based scheme, IET Gener. Transm. Distrib. 18 (4) (2024) 729–755.
- [16] Cleberton Reiz, Jonatas Boas Leite, Optimal coordination of protection devices in distribution networks with distributed energy resources and microgrids, IEEE Access 10 (2022) 99584–99594, http://dx.doi.org/10.1109/ACCESS.2022. 3203713.
- [17] Khaled A. Saleh, Hatem H. Zeineldin, Ehab F. El-Saadany, Optimal protection coordination for microgrids considering N-1 contingency, IEEE Trans. Ind. Inf. 13 (5) (2017) 2270–2278, http://dx.doi.org/10.1109/TII.2017.2682101.
- [18] Alexandre A. Kida, Angel E. Labrador Rivas, Luis A. Gallego, An improved simulated annealing-linear programming hybrid algorithm applied to the optimal coordination of directional overcurrent relays, Electr. Power Syst. Res. (ISSN: 0378-7796) 181 (2020) 106197, http://dx.doi.org/10.1016/j.epsr.2020.106197.
- [19] Soham Chakraborty, Sarasij Das, Communication-less protection scheme for AC microgrids using hybrid tripping characteristic, Electr. Power Syst. Res. (ISSN: 0378-7796) 187 (2020) 106453, http://dx.doi.org/10.1016/j.epsr.2020.106453.
- [20] Heba Beder, Baraa Mohandes, Mohamed Shawky El Moursi, Ebrahim A. Badran, Magdi M.El Saadawi, A new communication-free dual setting protection coordination of microgrid, IEEE Trans. Power Deliv. 36 (4) (2021) 2446–2458, http://dx.doi.org/10.1109/TPWRD.2020.3041753.

- [21] Katiani Pereira, Benvindo R. Pereira, Javier Contreras, José R.S. Mantovani, A multiobjective optimization technique to develop protection systems of distribution networks with distributed generation, IEEE Trans. Power Syst. 33 (6) (2018) 7064–7075, http://dx.doi.org/10.1109/TPWRS.2018.2842648.
- [22] Wandry R. Faria, Daniella de B. Martins, Ciniro A.L. Nametala, Benvindo R. Pereira, Protection system planning for distribution networks: A probabilistic approach, Electr. Power Syst. Res. (ISSN: 0378-7796) 189 (2020) 106612, http://dx.doi.org/10.1016/j.epsr.2020.106612.
- [23] Cleberton Reiz, Jonatas B. Leite, Clara S. Gouveia, Mohammad Sadegh Javadi, Protection system planning in distribution networks with microgrids using a bi-level multi-objective and multi-criteria optimization technique, Electr. Power Syst. Res. (ISSN: 0378-7796) 228 (2024) 109966, http://dx.doi.org/10.1016/j. epsr.2023.109966.
- [24] Wandry Rodrigues Faria, Ciniro Aparecido Leite Nametala, Benvindo Rodrigues Pereira Jr., Cost-effectiveness enhancement in distribution networks protection system planning, IEEE Trans. Power Deliv. 37 (2) (2022) 1180–1192, http://dx.doi.org/10.1109/TPWRD.2021.3079926.
- [25] Wandry R. Faria, Etiane O.P. Carvalho, Luciano B. Dantas, Carlos D. Maciel, Luís F.C. Alberto, João B.A. London Jr., Benvindo R. Pereira Jr., Service restoration in modern distribution systems addressing grid-connected and islanded operations, Electr. Power Syst. Res. 196 (2021) 107238.
- [26] Wandry R. Faria, Mario Oleskovicz, Denis V. Coury, Rodrigo B. Otto, Benvindo R. Pereira, Intentional Island and dynamic analysis of a micrognd, in: 2019 IEEE Milan PowerTech, 2019, http://dx.doi.org/10.1109/PTC.2019.8810559.

- [27] G. Benmouyal, M. Meisinger, J. Burnworth, W.A. Elmore, K. Freirich, P.A. Kotos, P.R. Leblanc, P.J. Lerley, J.E. McConnell, J. Mizener, J. Pinto de Sa, R. Ramaswami, M.S. Sachdev, W.M. Strang, J.E. Waldron, S. Watansiriroch, S.E. Zocholl, IEEE standard inverse-time characteristic equations for overcurrent relays, IEEE Trans. Power Deliv. (ISSN: 0885-8977) 14 (3) (1999) 868–872, http://dx.doi.org/10.1109/61.772326.
- [28] Vassilis Kekatos, Liang Zhang, Georgios B. Giannakis, Ross Baldick, Voltage regulation algorithms for multiphase power distribution grids, IEEE Trans. Power Syst. 31 (5) (2016) 3913–3923, http://dx.doi.org/10.1109/TPWRS.2015. 2493520
- [29] Georgios B. Giannakis, Vassilis Kekatos, Nikolaos Gatsis, Seung-Jun Kim, Hao Zhu, Bruce F. Wollenberg, Monitoring and optimization for power grids: A signal processing perspective, IEEE Signal Process. Mag. 30 (5) (2013) 107–128, http://dx.doi.org/10.1109/MSP.2013.2245726.
- [30] Wandry Rodrigues Faria, Gregorio Muñoz-Delgado, Javier Contreras, Benvindo Rodrigues Pereira Jr., Eletronic companion A novel MILP formulation for optimal allocation and coordination of protective and switching devices in active distribution networks, 2024, URL http://dx.doi.org/10.5281/zenodo.13851601.
- [31] Gurobi Optimization, LLC, Gurobi optimizer reference manual, 2023, URL https://www.gurobi.com.
- [32] R. Fourer, D.M. Gay, B.W. Kernighan, AMPL: A Modeling Language for Mathematical Programming, second ed., Thomson, Duxbury, MA, USA, ISBN: 9780534388096, 2003.